

腮腺基底细胞腺瘤MRI特征与病理对照 分析

何慕真¹, 张盛箭², 马明平¹, 黄海建³

1. 福建医科大学省立临床学院, 福建省立医院放射科, 福建 福州 350000;
2. 复旦大学附属肿瘤医院放射诊断科, 复旦大学上海医学院肿瘤学系, 上海 200032;
3. 福建医科大学省立临床学院, 福建省立医院病理科, 福建 福州 350000

[摘要] **背景与目的:** 腮腺基底细胞腺瘤(basal cell adenoma, BCA)发病率相对较低, 临床误诊率高, 目前为止, 对该病的MRI表现报道较少。该研究结合动态增强磁共振成像(dynamic contrast enhanced magnetic resonance imaging, DCE-MRI)和扩散加权成像(diffusion weighed imaging, DWI)探讨BCA的MRI特征及其与病理学相关性。**方法:** 回顾性分析经手术病理证实的26例腮腺BCA患者的临床表现、病理学改变及MRI影像学特征。分析患者临床表现、病灶数目、部位、大小、形态、信号与强化特征及其病理学表现。**结果:** 26例患者中, 女性18例; 中位年龄51(32~72)岁; 共27枚病灶(25例单发, 1例双侧各1枚)。病灶平均大小22 mm(11~36 mm)。13枚病灶位于浅叶, 5枚位于深叶, 9枚同时累及深、浅叶; 肿瘤呈圆形或椭圆形, 均未见分叶, 边界清楚, 其中25枚病灶T2WI见周缘低信号环; 对照颈部肌肉, 病灶实性部分T1WI呈等或略高信号, T2WI呈高或略高信号, 其中21枚病灶内见大小不一囊变区。增强后21枚病灶实性部分呈均匀强化, 6枚呈不均匀强化。时间-信号强度曲线显示21枚病灶(77.8%)呈平台型, 6枚(22.2%)呈流出型。9例患者(10枚病灶)行DWI检查, 表现弥散系数图(apparent diffusion coefficient, ADC)均值为 $(1.22\pm 0.20)\times 10^{-3}$ mm²/s。镜下显示: 肿瘤由单一基底细胞构成, 并有明显的基底细胞层及基底膜样结构, 缺乏黏液软骨样成分。**结论:** 腮腺BCA的MRI表现有一定特征性, 分析其MRI特征与其病理相关性, 对于肿瘤的定性诊断及鉴别诊断有较大的价值。

[关键词] 腮腺; 基底细胞腺瘤; 磁共振成像; 病理学

DOI: 10.19401/j.cnki.1007-3639.2017.12.003

中图分类号: R738.87 文献标志码: A 文章编号: 1007-3639(2017)12-0935-05

MRI features of basal cell adenoma of the parotid gland and its correlation with pathology HE Muzhen¹, ZHANG Shengjian², MA Mingping¹, HUANG Haijian³ (1. Provincial Clinical College, Fujian Medical University, Department of Radiology, Fujian Provincial Hospital, Fuzhou 350000, Fujian Province, China; 2. Department of Radiology, Fudan University Shanghai Cancer Center, Department of Oncology, Shanghai Medical College, Fudan University, Shanghai 200032, China; 3. Provincial Clinical College, Fujian Medical University and Department of Pathology, Fujian Provincial Hospital, Fuzhou 350000, Fujian Province, China)

Correspondence to: ZHANG Shengjian E-mail: zhangshengjian@yeah.net

[Abstract] **Background and purpose:** Basal cell adenoma (BCA) of the parotid gland has low incidence and high misdiagnosis rate in clinical practice. So far, the report on the MRI manifestation of BCA is rare. Our study combined dynamic contrast enhanced magnetic resonance imaging (DCE-MRI) with diffusion weighed imaging (DWI) to investigate the MRI features of BCA of the parotid gland and its correlation with pathologic features. **Methods:** We retrospectively analyzed the correlation of MRI findings and pathology in 26 patients with histopathologically proven BCA of the parotid gland. The clinical presentation, pathologic features and localization, size, number, shape, signal, enhancement pattern of tumor were analyzed. **Results:** In this study, 18 patients (69.2%) were female and 8 patients (30.8%) were male. The median age was 51 (range 32-72) years. Twenty-five patients (96.2%) had single

lesion and only one patient (3.8%) had two. The average size of the 27 lesions was 22 (range 11-36) mm. Thirteen lesions were located in superficial lobe, 5 in deep lobe and 9 across both lobes. All the 27 lesions had clear margin without lobular appearance and 25 lesions had complete or incomplete hypo-intensity rim in T2WI. Compared with neck muscle, all 27 lesions showed iso- or hyper-intense in T1WI and hyper-intense in T2WI. Twenty-one lesions (77.8%) had cystic change with varying size. The signal intensities of solid part of lesions were homogeneous in 21 lesions, heterogeneous in 6. Twenty-one lesions (77.8%) showed persistent enhancement and 6 (22.2%) had outflow enhancement. DWI was performed in 9 patients (10 lesions), the mean ADC value was $(1.22 \pm 0.20) \times 10^{-3} \text{ mm}^2/\text{s}$. Under microscope, it consisted of a monomorphic population of basaloid epithelial cells, organized with prominent basal cell layer and distinct basement membrane-like material, lacking the myxochondroid stromal component. **Conclusion:** BCA of the parotid gland has certain clinical and MRI features. Analysis of the correlation between the MRI findings and the pathologic features may be helpful in making qualitative and differential diagnosis of BCA.

[**Key words**] Parotid gland; Basal cell adenoma; Magnetic resonance imaging; Pathology

基底细胞腺瘤(basal cell adenoma, BCA)是一种少见的良性涎腺上皮性肿瘤, 80%发生在腮腺, 仅占腮腺肿瘤的1%~3%^[1]。由于该病发病率相对较低, 临床误诊率高。目前为止, 对该病的MRI表现报道较少, 而关于BCA的动态增强磁共振成像(dynamic contrast enhanced magnetic resonance imaging, DCE-MRI)和扩散加权成像(diffusion weighed imaging, DWI)的影像学特征目前尚缺乏相关报道。本研究回顾性分析26例经手术病理证实的腮腺BCA的临床与DCE-MRI及DWI特征, 分析该特征与病理诊断结果的相关性, 旨在提高影像诊断医师对该疾病的诊断及鉴别诊断能力。

1 资料和方法

1.1 一般资料

回顾性分析福建省立医院及复旦大学附属肿瘤医院26例经手术病理证实的腮腺BCA患者, 其中男性8例, 女性18例, 男女比例1:2.3; 中位年龄51岁(32~72岁), 40岁以下的患者有3例(11.5%), 40~60岁有14例(53.8%, 其中女性10例), 60~70岁有8例(30.8%), 70岁以上者1例(3.8%)。平均病程长43个月, 其中3例超过10年。26例患者均为偶然发现耳下肿块就诊, 其中有2例有肿物近期迅速增大病史。除2例患者伴有隐痛外, 其他均无明显临床症状。体格检查中仅1例病灶有压痛, 余均无压痛触痛; 5例活动度较差, 余患者活动度尚可; 9例质韧、1例质软, 其余均为质地中等。本组中有长期吸

烟史者3例(11.5%), 均为男性患者, 烟龄20~30年, 日吸烟15~20支。

1.2 检查方法

17例MR检查采用GE Signal 1.5T MRI扫描仪, 扫描序列: 行SE或FSE序列进行轴面T1WI(TR 500~660 ms, TE 15~30 ms)和T2WI(TR 2 000~4 500 ms, TE 60~128 ms)扫描, 层厚3~4 mm, 层距3 mm, 辅以冠状面T2WI, 增强序列采用横断面SE T1WI多期动态扫描6~8次。9例MR检查采用Siemens Aera 1.5T MRI扫描仪, 扫描序列: 常规行横轴位T1WI(TR 600 ms, TE 10 ms), 横轴位及冠状位T2WI(TR 2 500 ms, TE 80 ms), FS T2WI(TR 2 800 ms, TE 83 ms)扫描, 层厚4 mm, 层间距0.8 mm, 辅以及冠状T2WI-TIRM(turbo inversion recovery magnitude, TIRM)(TR 3 000 ms, TE 39 ms, TI 220 ms)。DWI采用单次激发自旋回波(EPI)序列(TR 6 800 ms, TE 82 ms), 扩散敏感系数(*b*值)采用0、500及1 000 s/mm²。动态增强采用三维容积内插快速扰相梯度回波序列(volumetric interpolated breath-hold examination, VIBE), 共采集28组动态增强图像。对比剂采用钆喷替酸葡甲胺(Gd-DTPA), 剂量0.1 mmol/kg。时间-信号强度曲线(time-signal intensity curve, TIC)选择强化最明显的区域为感兴趣区(region of interest, ROI), 避开肉眼可见的出血、液化、坏死及囊变。

1.3 影像评估

由2位从事MRI颈部影像诊断方向的影像医师(1名主治医师, 1名主任医师)对所有患者MRI

影像学资料进行独立分析,根据肿块位置将其分组,浅叶与深叶以下颌后静脉为界,前、后部以腮腺最大横轴面前后径中点为界划分:浅叶内肿瘤为第1组,发生于腮腺深叶的为第2组,同时累及浅、深叶为第3组。分析内容包括肿瘤的部位、数量、大小、形态、边界、肿瘤信号特点、强化方式和表观弥散系数图(apparent diffusion coefficient, ADC)值。DCE-MRI采用的Yabuuchi等^[2]的分型,将曲线分4种类型:

A型:持续上升型;B型:廓清型(速升速降型),强化快速达最高值后快速下降(廓清率大于30%);C型:即较快上升后处于平稳状态(廓清率小于30%);D型:平线型,即处于基线水平,组织无明显强化。

2 结 果

2.1 肿瘤数目、部位及大小

25例为单发病灶,1例为双侧腮腺各1枚,其中15枚病灶位于左侧,12枚病灶位于右侧。全部27枚病灶大小为11~36 mm,平均值为 (22.2 ± 7.4) mm,其中4枚病灶最大径

大于30 mm。1组病灶13枚,其大小平均值为 (18.6 ± 7.3) mm;两组病灶5枚其大小平均值为 (22.5 ± 5.1) mm;3组病灶9枚,其大小平均值为 (31.7 ± 4.2) mm。此外,位于浅叶的13枚病灶,仅有2例位于腮腺前部,其余11例均位于腮腺后下部。

2.2 影像学特征

27枚病灶形态均呈圆形或椭圆形,边界清楚。21枚病灶内可见大小不等片状、裂隙样囊变区(77.8%),较小的囊变区以病灶外周分布为主,大的囊变区累及病灶的中心及外周。与颈部肌肉对比,T1WI实性部分呈等或稍高信号,囊变区呈低或明显高信号;T2WI实性部分呈高或略高信号,但低于周围正常腮腺实质信号,囊变、坏死区呈明显高信号。25枚病灶(92.5%)周围均可见环状T2WI低信号包膜,其中20枚病灶包膜完整,5枚病灶包膜不完整。21枚病灶(77.8%)实性部分呈均匀强化,6例(22.2%)呈不均匀强化,囊变区无强化。动态增强扫描中6例呈B型曲线(22.2%),21例呈C型曲线(77.8%),未见A、D型曲线。10枚病灶行DWI序列检查,ADC均值为 $(1.22 \pm 0.20) \times 10^{-3} \text{ mm}^2/\text{s}$ (图1)。

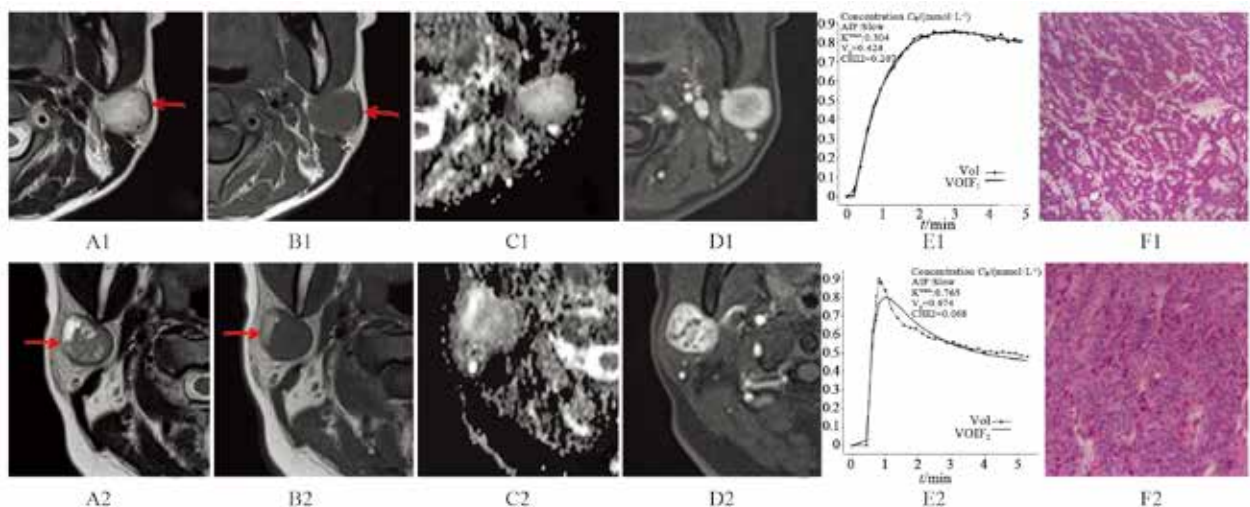


图1 两例患者的MRI图像、TIC曲线及病理诊断结果

Fig. 1 The MRI diagnosis, TIC curves and pathological diagnosis of 2 BCA patients

A1-E1: Female patient, 32-year-old, a mass under the left ear was found. The lesion had clear margin without lobular appearance, was located across superficial and deep lobe of the left parotid gland. Compared with neck muscle, the lesion showed iso-intense in T1WI, hyper-intense in solid portion with hypo-intensity rim in T2WI and persistent enhancement in the DCE-MRI. The mean ADC value was $1.18 \times 10^{-3} \text{ mm}^2/\text{s}$; A2-E2: Female patient, 49-year-old, a palpable mass was found in the right parotid region 15 days ago. MRI showed a round, well-defined mass located across superficial and deep lobe of the right parotid gland with large cystic change and homogeneous enhancement. The lesion showed outflow enhancement in the DCE-MRI. The mean ADC value was $1.09 \times 10^{-3} \text{ mm}^2/\text{s}$; F1, F2: Under microscope(H-E, $\times 100$), the tumor was consist of a monomorphic population of basaloid epithelial cells, organized with prominent basal cell layer and distinct basement membrane-like material

2.3 组织病理学特征

大体标本上, 肿瘤呈实性, 20枚病灶可见完整包膜, 5枚病灶可见不完整包膜, 周围可见涎腺组织。切面肿瘤灰白至灰褐色, 无黏液感, 质中等或韧, 界限清, 21枚病灶内见囊变。镜下肿瘤由单一基底细胞构成, 细胞质嗜酸性, 界不清或尚清, 细胞核圆形至椭圆形。瘤细胞呈岛状、栅栏样排列, 瘤细胞巢见多少不等的胶原纤维。部分瘤细胞呈梁状、索状排列, 间质见较多增生血管, 并水肿变性。免疫组织化学检测结果显示, 肿瘤细胞对角蛋白、肌源性标志、波形蛋白和p63呈阳性。

3 讨 论

BCA于1967年由Kleinsasser和Klein首先报道, 并将其列为涎腺肿瘤的一个类型。1991年WHO将BCA归类为单形性腺瘤的一种亚型。2005年, WHO将BCA定义为: 由单一基底样形态的肿瘤细胞构成, 并有明显的基底细胞层及基底膜样结构, 缺乏多形性腺瘤中的黏液软骨样成分^[1]。组织学上肿瘤分成4种亚型: 实体型、管状型、梁状型和膜性型。BCA主要的治疗方式为肿瘤局部切除术, 无需行腮腺浅叶切除。膜性型BCA复发率高(24%), 实体型、管状型、梁状型复发可能性极小, 可能与膜性型病灶呈多中心性有关, 且膜性型较其他型更容易恶变^[3]。

BCA的平均发病年龄为57.7岁, 男女之比为1:2^[4]。本组26例中位年龄为51岁, 男性与女性之比为1:2.3, 40~60岁占半数以上(53.8%), 比多形性腺瘤平均好发年龄大10岁左右, 与文献报道基本相符。临床上多表现为无痛性渐大肿块, 病史较长, 本组中平均病程为43个月, 符合良性肿瘤生长方式, 临床触诊肿块活动度好, 质地中等, 与周围组织无明显黏连。本组中仅有3例患者(占11.5%)有长期吸烟史, 且为中老年男性, 提示BCA可能与吸烟的相关性不大。

BCA影像学表现及其与病理学相关性: BCA形态呈圆形及椭圆形, 未见分叶状病灶,

肿块边界清楚, 本组中25枚(92.6%)病灶在T2WI上可见周围环状低信号, 这与大体标本上可见肿块周围纤维包膜结构相符^[4]。本组85%的肿块小于30 mm, 肿瘤无特定好发部位, 本研究中发生于腮腺浅叶的比例稍高, 占48.0%, 可能是由于浅叶病灶易于触及, 而早期发现就诊, 25例(96.1%)为单发病灶。肿瘤实性部分富含细胞结构且排列紧密, 此外, 缺乏黏液软骨样成分, 故其T2WI信号较多形性腺瘤低。本研究中77.8%的肿块内可见囊变或裂隙状无强化区, 大的囊变多位于病灶中心, 可能于肿瘤内出血有关, 而小片状、裂隙状无强化灶多位于病灶周围, 从包膜向肿瘤内部延伸, 镜下主要是胶原软骨成分^[1]。Jang等^[4]认为病灶内囊变区与病灶大小无关, 即使较小的病灶内也可以出现囊变。本组中最小的直径11 mm病灶亦出现片状、裂隙样囊变区。MRI动态增强早期, 对比剂主要分布于血管内, 信号强度与肿瘤血管生成程度有关; 动态增强晚期, 对比剂分布于细胞外间隙, 与微血管通透性和密度有关^[5]。本研究27例病灶通过增强扫描发现在肿瘤早期即明显强化, 病理诊断发现, 镜下肿瘤富含特征性沿内皮排列的血管网, 同时伴有基底细胞巢围成小管状结构, 在一定程度上影响了肿瘤早期强化。这些血管网主要是小静脉及毛细血管, 容易引起出血, 增强后未出现强化区^[1]。本组患者TIC曲线主要以B、C型为主, 未见A、D型曲线。Lee等^[6]认为肿瘤两种不同强化方式与主要与BCA不同细胞类型的细胞外基质含量有关。实体型肿瘤镜下血供丰富, 早期强化明显, 而瘤体内细胞分布密集, 细胞外间隙少, 因此, 延迟期造影剂迅速廓清。而管状型及梁状型肿瘤由于存在囊变区旁的黏液样变区, 这一病理改变造成肿块实性部分细胞分布较少, 细胞外间隙增大, 对比剂停留时间长。Mukai等^[7]报道的14例BCA的ADC值为 $(1.24 \pm 0.18) \times 10^{-3} \text{ mm}^2/\text{s}$, 与本研究的患者ADC值相符, 介于既往文献报道的多形性腺瘤ADC值 $[(1.74 \pm 0.37) \times 10^{-3} \text{ mm}^2/\text{s} \sim (2.14 \pm 0.11) \times 10^{-3} \text{ mm}^2/\text{s}]$ 与腺淋巴瘤ADC值 $[(0.85 \pm 0.10) \times 10^{-3} \text{ mm}^2/\text{s} \sim$

$(0.97 \pm 0.16) \times 10^{-3} \text{ mm}^2/\text{s}$] 范围之间^[7-10]。推测其原因, MR-DWI主要反映出组织中水分子弥散情况, 而水分子的弥散受到周围组织结构的影响。腺淋巴瘤由含高浓度黏液小囊样结构, 含蛋白的结合水扩散明显受限, 致其ADC值明显减低; 多形性腺瘤则由多种上皮结构、黏液间质及软骨基质构成, 水分子扩散受限不明显。BCA实性部分细胞成分较多形性腺瘤密集, 又缺乏腺淋巴瘤的高浓度黏液蛋白结构, 这些组织学特点可能决定了BCA的ADC值范围。由于BCA的发病率低, 本组患者数较少, 未对肿瘤进行具体病理分型, 对肿瘤内囊变形态及动态曲线差异。且本研究中行DWI检查患者数较少, 本组中ADC值对BCA影像诊断的价值有限, 有待于日后增加患者数, 再结合高清弥散加权成像(RESOLVE-DWI)进一步探讨。

腮腺BCA主要需与腮腺最常见两种良性上皮性肿瘤多形性腺瘤和腺淋巴瘤进行鉴别。

综上, 腮腺BCA发病率低, 临床容易误诊, 其临床特征及MRI影像学表现有一定鉴别诊断意义。对于中老年女性, 发现腮腺区无痛性肿块, MRI上呈单发, 形态清楚的圆形或椭圆形肿块, 周围有明显T2WI低信号包膜, 内部可见特征性片状、裂隙状囊变区, TIC呈廓清型或平台型曲线, ADC值介于腺淋巴瘤与多形性腺瘤间, 需考虑BCA可能。

[参 考 文 献]

[1] SHI L, WANG Y X, YU C, et al. CT and ultrasound features of basal cell adenoma of the parotid gland: a report of 22 cases

with pathologic correlation [J]. *AJNR Am J Neuroradiol*, 2012, 33(3): 434-438.

- [2] YABUUCHI H, FUKUYA T, TAJIMA T, et al. Salivary gland tumors: diagnostic value of gadolinium-enhanced dynamic MR imaging with histopathologic correlation [J]. *Radiology*, 2003, 226(2): 345-354.
- [3] OKAHARA M, KIYOSUE H, MATSUMOTO S, et al. Basal cell adenoma of the parotid gland: MR imaging findings with pathologic correlation [J]. *AJNR Am J Neuroradiol*, 2006, 27(3): 700-704.
- [4] JANG M, PARK D, LEE S R, et al. Basal cell adenoma in the parotid gland: CT and MR findings [J]. *AJNR Am J Neuroradiol*, 2004, 25(4): 631-635.
- [5] LEE F K, KING A D, MA B B, et al. Dynamic contrast enhancement magnetic resonance imaging (DCE-MRI) for differential diagnosis in head and neck cancers [J]. *Eur J Radiol*, 2012, 81(4): 784-788.
- [6] LEE D K, CHUNG K W, BAEK C H, et al. Basal cell adenoma of the parotid gland: characteristics of 2-phase helical computed tomography and magnetic resonance imaging [J]. *J Comput Assist Tomogr*, 2005, 29(6): 884-888.
- [7] MUKAI H, MOTOORI K, HORIKOSHI T, et al. Basal cell adenoma of the parotid gland: MR features and differentiation from pleomorphic adenoma [J]. *Dentomaxillofac Radiol*, 2016, 45(4): 20150322.
- [8] HABERMANN C R, GOSSRAU P, GRAESSNER J, et al. Diffusion-weighted echo-planar MRI: a valuable tool for differentiating primary parotid gland tumors? [J]. *Rofo*, 2005, 177(7): 940-945.
- [9] YERLI H, AGILDERE A M, AYDIN E, et al. Value of apparent diffusion coefficient calculation in the differential diagnosis of parotid gland tumors [J]. *Acta Radiol*, 2007, 48(9): 980-987.
- [10] HABERMANN C R, ARNDT C, GRAESSNER J, et al. Diffusion-weighted echo-planar MR imaging of primary parotid gland tumors: is a prediction of different histologic subtypes possible? [J]. *AJNR Am J Neuroradiol*, 2009, 30(3): 591-596.

(收稿日期: 2017-07-12 修回日期: 2017-10-31)